Computational Micromechanics of Particle-reinforced Composites: Effect of Complex Three-dimensional Microstructures

Liu-Juan Zhu*
Shanghai Institute of Technology, Shanghai 200235, China
E-mail: zhulj@sit.edu.cn

Wen-Zhong Cai
Nanjing University of Technology, Nanjing 210009, China
E-mail: wzcai@njut.edu.cn

Shan-Tung Tu
East China University of Science and Technology, Shanghai 200237, China
Nanjing University of Technology, Nanjing 210009, China
Email: sttu@ecust.edu.cn

Abstract—**It is of interest to incorporate quantitative characterization of actual three-dimensional microstructures in micromechanical analysis of composites due to the dominant influence of microstructural features on the material behavior. In this paper, a methodology has been developed to perform finite element-based simulations on complex three-dimensional microstructures, through its application to the aluminum matrix composites reinforced with randomly distributed SiC particles of highly variable and irregular geometries. The effect of the complex microstructures on the micromechanics of the composites is investigated in terms of their elasto-plastic deformation and damage initiation. For comparison, the conventional simulations on the simplified microstructures, i.e., randomly distributed spheroids, are also carried out. The difference is significant between the simulation results based on the complex microstructures and on the simplified ones, respectively. Confirmed by available experimental data, it is believed that the computational micromechanics capturing the complex features of realistic microstructure provides a more accurate and comprehensive picture for predicting and understanding the material behavior of particle-reinforced composites. The present methodology is also efficient to represent the virtual complex microstructures and hence promising for the design and application of composites.**

Index Terms—**microstructure, micromechanics, simulation, finite element method, particle-reinforced composites**

I. INTRODUCTION

A thorough understanding of microstructure and its effect on macroscopic properties is essential for the design and development of high-performance composite materials. This is particularly challenging for the particle-reinforced composites due to their realistic complex microstructures. Incorporating the actual 3D microstructures of the composites is crucial for obtaining an accurate prediction of material behavior. The classical analytical models [1–4] and conventional numerical modeling [5–10] often fail to match precisely with the experimentally observed behavior of the composites because they approximate the highly variable and irregular angular structure of particles using simplified particle geometries such as spheres or ellipsoids. Recently, some 3D experimental visualization techniques, such as serial sectioning [11–13], X-ray tomography [14] and holotomography [15,16], have been developed to reconstruct the actual microstructures of the composites. The experimental visualization from the prepared composites is generally reliable but burdensome for property prediction and material design.

As an alternative, an efficient and flexible computer simulation that captures complex morphologies of the realistic particles may be preferable. However, it is questionable for the existing simulations to reproduce the actual microstructures of the particle-reinforced composites. They usually forbid particle overlapping using the minimum distance between neighboring particles [5]. This geometrical test can be implemented in a straightforward way for spherical particles, and become a fairly complex task for randomly dispersed and oriented cylinders or ellipsoids [5]. But it is too complicated for the realistic complex particles and loses its practical applicability. Therefore, establishing an efficient approach to deal with the geometrical interaction is particularly challenging for the computer simulations of the actual microstructures of particle-reinforced composites.

In this contribution, we develop a three-dimensional (3D) microstructure-based simulation of the particle-reinforced composites to capture the complex characteristics in their realistic microstructures. Its

* Corresponding author: zhulj@sit.edu.cn

doi:10.4304/jcp.4.12.1237-1242

application to the microstructure reconstruction of 2080 aluminum alloy matrix composites reinforced with SiC particles of highly variable and irregular geometries is presented and followed by a finite element modeling of the micromechanical behavior and macroscopic response of the composites.

II. MICROSTRUCTURE-BASED SIMULATION

To perform a microstructure-based simulation, some typical particles of realistic morphology are first generated. Then, these particles are embedded into in a cubic unit cell. Their positions and orientations are initiated randomly and accepted selectively and sequentially. No particle overlapping is permitted. If the surface of the particle cuts any of the cubic unit cell surfaces, this condition is checked with the particles near the opposite surface because of the periodic microstructure of the composite. The present simulation follows the voxel technique [17] and the particles are discretized and digitized. The particle overlapping is directly judged by the Boolean operations between the surface voxels of the different particles. It takes no account of the minimum distance between neighboring particles. It is hence appropriate for incorporating the complex morphologies of realistic particles. To automatically generate a representative volume element for the micromechanical modeling, an ASCII file based on the above algorithm is created as an input to the preprocessor of ANSYS (Ansys Inc., Canonsburg, PA, 2004). The present simulation is illustrated as follows, by its application to the microstructure of highly variable and irregular SiC particle reinforced composites [12,13,16].

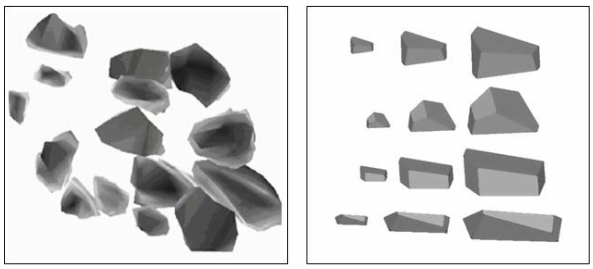

Figure 1. Realistic morphology (left) versus simulated structure (right) of SiC particles.

As shown in Figure 1, from the realistic particle morphology, the simulated particles of four different shapes each with three different sizes are summarized statistically to capture the nature of complex irregularity and angularity. For simplicity, this simulation is not an exact description of the realistic particles. The total particle number is taken a relatively small value of 24. Nevertheless, a rigorously matched microstructure will be reproduced if more information about actual morphology and more particles are included at a given particle volume fraction. Using these simulated particles, a microstructure-based model for SiC particle reinforced composites is shown in Figure 2. The particle volume fraction is 20%. For comparison, a simplified-particle model is also given in Figure 2. It includes the spheres and ellipsoids of the same volumes, aspect ratios, locations and orientations as the exactly corresponding particles of complex morphologies.

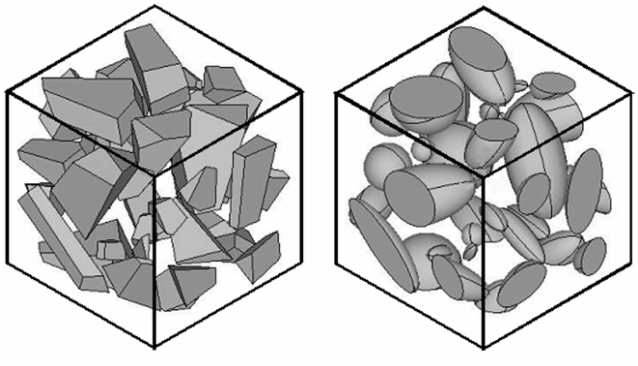

Figure 2. Microstructure-based model (left) versus simplified-particle model (right) with periodic boundary conditions.

In addition, it is convenient to extend this technique to the non-uniform (e.g., clustering and graded) and anisotropic microstructure simulations when some non-uniform random functions are used for particle distribution and orientation. This reflects the effect of process parameters on the microstructure. Therefore, it is believed that the present computer simulation is available for a reliable and flexible representation of the virtual complex microstructure via different combinations of process parameters.

III. FINITE ELEMENT MODELING

The finite element modeling on the simulated unit cells is performed with ABAQUS/Standard (Hibbit, Karlsson and Sorensen Inc., Pawtucket, RI, 2004) within the framework of small displacements theory. The modified 10-node tetrahedral elements are employed to avoid possible volume locking in yielded matrix regions. A standard model contains approximately 80,000 elements and 110,000 nodes. The perfect particle/matrix interface is assumed. The SiC particles are isotropic and elastic (Young's modulus 410 GPa and Poisson's ratio 0.19). The experimentally determined stress-strain curve for the aluminum alloy [16] is used to the input of the matrix. The Young's modulus and Poisson's ratio of the Al alloy are 74 GPa and 0.33. Three different realizations are generated for the microstructure-based model and the simplified-particle model, respectively. Each of them is subjected to uniaxial tensile strain (4%) along the three concurrent edges of the cube. The average stress-strain curve is separately determined for the microstructure-based model and simplified-particle model. Periodic boundary conditions are applied to the unit cell faces. If three concurrent edges of the cube stand for the axes of coordinates x_1, x_2, and x_3, the periodic boundary conditions can be expressed as a function of the displacement vector **u** as

$$\begin{aligned}\mathbf{u}(x_1, x_2, 0) - \mathbf{u}_3 &= \mathbf{u}(x_1, x_2, L)\\ \mathbf{u}(x_1, 0, x_3) - \mathbf{u}_2 &= \mathbf{u}(x_1, L, x_3)\\ \mathbf{u}(0, x_2, x_3) - \mathbf{u}_1 &= \mathbf{u}(L, x_2, x_3)\end{aligned} \quad (1)$$

where L is the edge length of the cube, and the displacements $\mathbf{u}_1$, $\mathbf{u}_2$, and $\mathbf{u}_3$ depend on the particular loading applied on the unit cell. For instance, tensile loading along the x_3 axis is obtained with $\mathbf{u}_3(0,0,u)$, $\mathbf{u}_1(u_1,0,0)$, and $\mathbf{u}_2(0,u_2,0)$, and u_1 and u_2 being computed from the conditions

$$\begin{aligned}\int_\Omega \sigma_1 \mathrm{d}\Omega = 0 \quad \text{on} \quad x_1 = L\\ \int_\Omega \sigma_2 \mathrm{d}\Omega = 0 \quad \text{on} \quad x_2 = L\end{aligned} \quad (2)$$

where σ_1 and σ_2 stand for the normal tractions acting on the cell faces contained, respectively, in the planes $x_1=L$ and $x_2=L$, and Ω represents the actual cross-section of each face. The applied strain along the x_3 axis is given by $\varepsilon_3=u/L$ and the corresponding stress is obtained as the total load acting on the cell face $x_3=L$, divided by the actual cross-section of this face.

IV. Results and Discussion

A. Macroscopic response and micromechanics

The advantage of using a 3D microstructure-based model is first shown by a comparison of the simulated stress-strain curve with the related experimental results [16], and the 3D simplified-particle modeling. As shown in Figure 3, the microstructure-based model predicts the experimental behavior quite well. The simplified-particle model underestimates the experimental results.

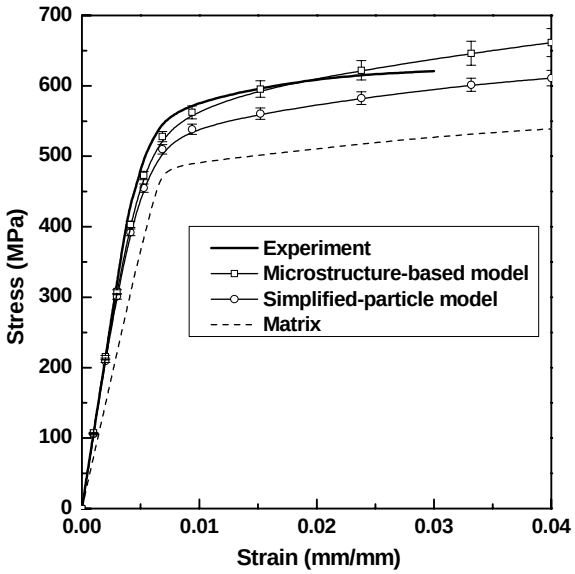

Figure 3. Comparison of the experimental and simulated stress-strain curves.

To better understand the effect of realistic complex microstructure on the macroscopic properties, the micromechanical field is also investigated. As shown in Figure 4(a), the maximum principal stress in the

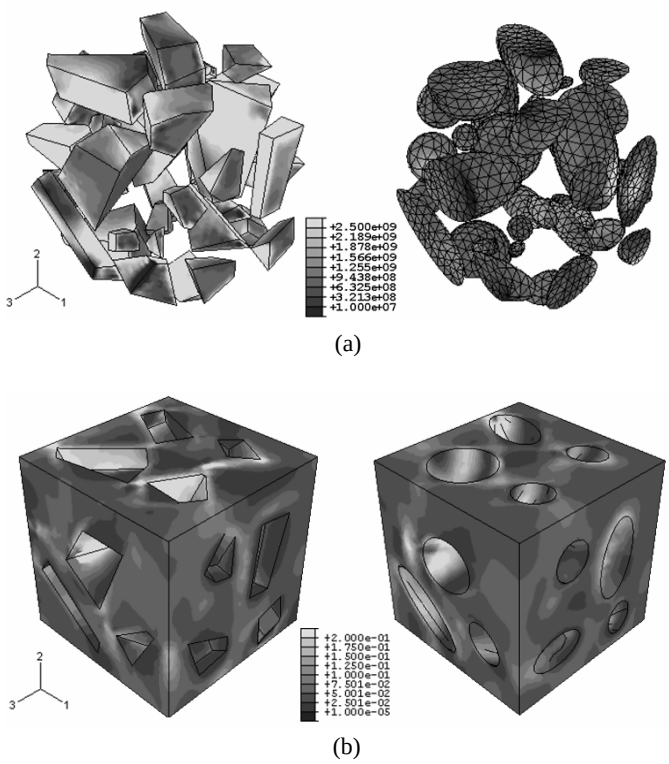

Figure 4. Contour plot of (a) maximum principal stresses in the particles, and (b) equivalent plastic strains in the matrix at a far-field axial strain of 4% in the 1-axis direction for microstructure-based model (left) and simplified-particle model (right), respectively.

simplified particles is quite uniform, while that in the angular particles is not. The angular particles are under much a higher stress than the simplified particles, indicating more load transfer to the angular particles. This may explain the higher improvement of the elasto-plastic properties in the microstructure-based model. Figure 4(b) shows the equivalent plastic strain in the matrix. A more inhomogeneous plastic strain is observed in the microstructure-based model. The localized plasticity that results from the sharp and angular nature of SiC particles can only be captured by the microstructure-based model. These comparisons show that the realistic complex microstructure significantly affects the micromechanical fields and eventually the macroscopic properties.

Figure 5 gives the evolution of equivalent plastic strain in the 2D sections at the same locations of these two models. As expected, the local stresses and strains depend on the microstructural morphologies in a complex manner. Local maxima in these micromechanical fields appear in the matrix regions between particles closely packed along the deformation axis. Slight deviations from the deformation axis lead to a dramatic reduction in the levels of these fields in the matrix between the particles, even when they are very closely packed. The plastic deformation becomes concentrated at the poles of the particles along the loading axis, as predicted by Goodier [18]. Some bands are formed and oriented at approximately ±45° to the loading direction. It is also interesting to note that within a region where the particles are more closely spaced, there is a lack of plasticity due

to the large degree of constraint on the matrix in these regions. It is well shown in the evolution of equivalent plastic strain that the onset of plastic flow appears at sharp angular corners of the particles, followed by localization of strain between particles. The angularity of the particles induces the more serious plastic strain concentrations.

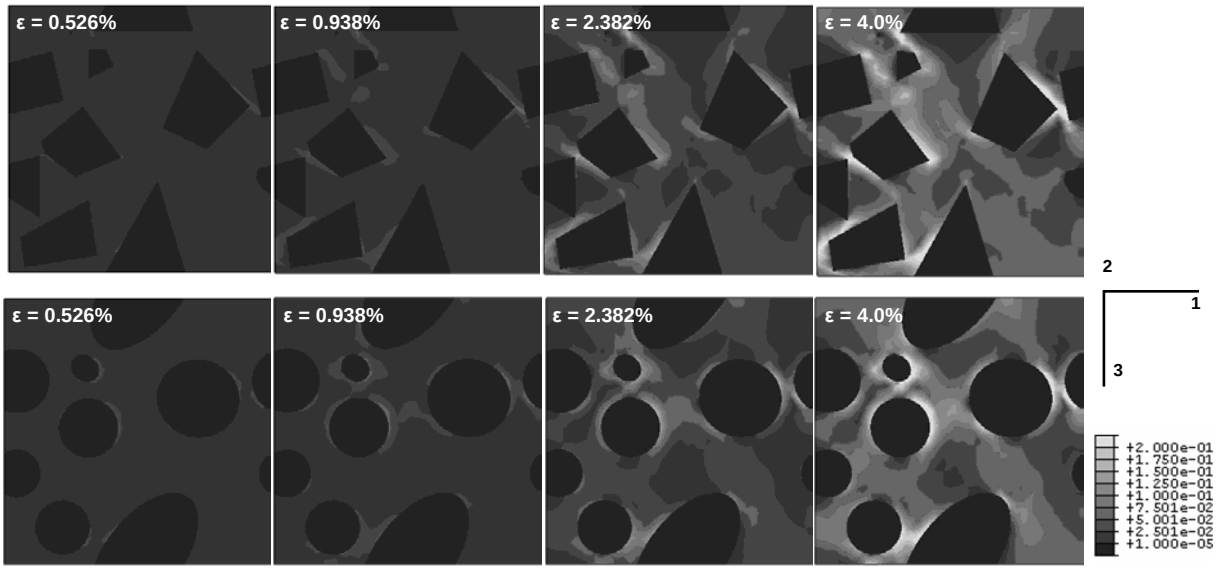

Figure 5. Contour plot of the equivalent plastic strain in the 2D sections at the same locations of microstructure-based model (top) and simplified-particle model (bottom), respectively. A far-field axial strain of 4% is applied in the 1-axis direction.

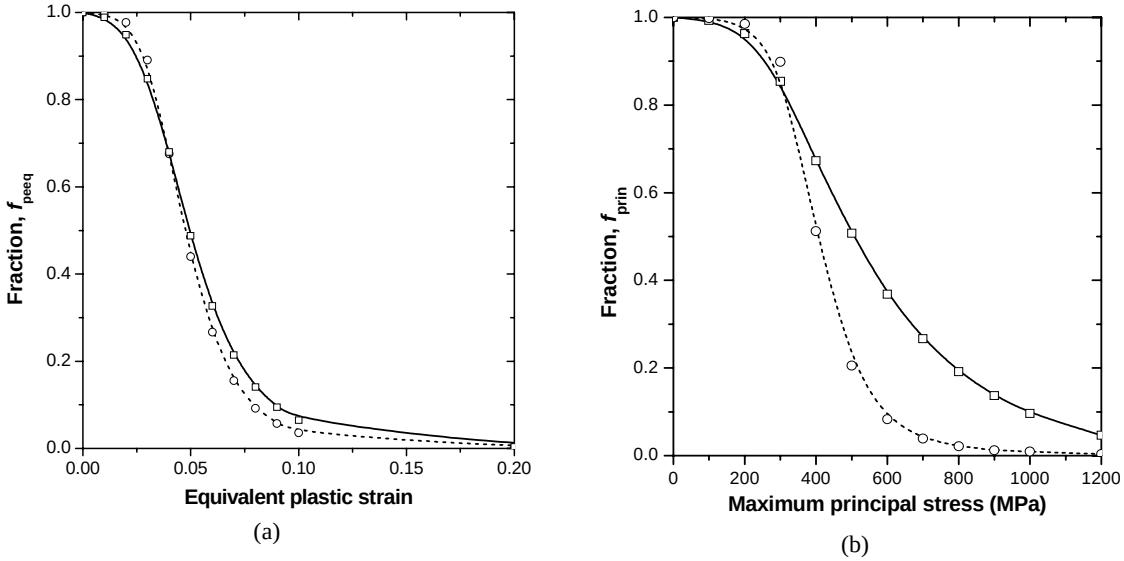

Figure 6. Comparisons of the ensemble averages of the fraction of matrix with a higher equivalent plastic strain (a) and of particles with a higher maximum principal stress (b) between the microstructure-based model (solid line) and simplified-particle model (dashed line) at a far-field axial strain of 4%.

High local stresses and/or strains are important factors in the study of the microstructure/macroscopic properties relationship, as well as in assessing the micromechanical failure of phase materials in the damage analysis. It is meaningful to analyze the extent of matrix and particles experiencing high local stresses and/or strains. A quantitative comparison of the local stress/strain distributions is conveniently done by analyzing the fraction of the element having the micromechanical fields higher than a given value. Fig. 6(a) compares the ensemble averages of the fraction of matrix f_{peeq} with a higher equivalent plastic strain ε_{peeq} between the microstructure-based model and simplified-particle model. It is found that the distributions of f_{peeq} are similar for these two models. However, the comparison of the ensemble averages of the fraction of particles f_{prin} with a higher maximum principal stress σ_{prin} between these two models shows marked difference, as shown in Fig. 6(b). It also indicates that realistic angular particles share much stronger reinforcing effect than the corresponding simplified particles.

B. Damage initiation

In the present composites there are three important mechanisms for initiating damage at the microscale. Their relative importance depends on the material system. They are the ductile damage of the matrix, the brittle cleavage of the particles, and the interfacial decohesion between matrix and particles. In view of much higher load transfer, the complex angular particles in turn have much higher fracture probabilities than the corresponding simplified particles. To obtain a quantitative difference of the particle brittle crack probability between the microstructure-based model and simplified-particle model, an assessment of the fracture probabilities of the particles is carried out in this work. The following study focuses on the damage mode of the particle crack. It is the dominant one for the material considered [19,20].

The fracture probabilities of the particles are assessed by a weakest link theory. Because Weibull's original approach [21] is formulated for brittle materials subjected to homogeneous uniaxial stress fields, it has to be modified to account for the fact that at the relevant volume fractions some multiaxiality and variability of the stresses is always present within each of the particles. The simplest Weibull-type model for such conditions gives the ensemble average value of the fracture probabilities of the particles, P_{ensemble}, as

$$P_{\text{ensemble}} = 1 - \exp\left[-\frac{1}{V_0} \int_{V_i:\sigma_1>0} \left(\frac{\sigma_1}{\sigma_f} \right)^m \mathrm{d}V \right] \qquad (3)$$

where σ_1 stands for the distribution of the maximum principal stress within the particle as obtained by the micromechanical analyses, V_i:σ_1>0 denotes the region of the particle for which this maximum principal stress is tensile, V_0 is a reference volume that is set equal to the particles' volume for the present study, and m = 3.0 and σ_f = 1.0 GPa are the Weibull modulus and the characteristic strength of the particles. Eq. (3) is expected to give reasonable results provided the stresses in the particles show only limited multiaxiality and no marked variation in the orientation of their principal stress axes (as is the case for overall uniaxial loading). The ensemble averages of particle fracture probabilities obtained from the microstructure-based model and simplified-particle model under the present applied load are equal to 10.5% and 35.6%, respectively. It means that the brittle fracture probabilities of the particles will be drastically underestimated if the realistic complex particles are replaced by the simplified particles in a micromechanical analysis.

Also note that the equivalent plastic strain and tensile hydrostatic stress are important micromechanical attributes for the matrix ductile failure in terms of the damage initiation and growth, respectively, while the maximum principal stress of particles is critical for the particle brittle cracking failure. Although the matrix-phase averages of these micromechanical fields in the microstructure-based model are very similar to those in the simplified-particle model, their local concentrations in the matrix around the sharp corners of the angular particles in the former are much more serious. The local damage mechanism in the matrix is sensitive to these concentrations, while the phase-average reinforcing effect in the composites is not. Hence, these concentrations result in the early damage initiations of the matrix at very low far-field strains. The damage initiations will be driven by high tensile hydrostatic stresses generated in the matrix region between particles aligned in the loading direction. Thus, it is expected that the effect of complex microstructures on the matrix damage is more significant than that of those simplified. The modeling and prediction of the local damage mechanism in the matrix of the composites with realistic complex microstructure is a considerably complex problem, which needs more effort in the future work.

V. Conclusions

In this work, the 3D microstructure-based simulation and deformation modeling of the particle-reinforced composites are studied, through its application to the aluminum alloy reinforced with SiC particles of highly variable and irregular geometries. The following conclusions can be made:

(1) A novel and efficient methodology is developed for computer simulations of 3D realistic microstructures of particle-reinforced composites. The simulations can incorporate realistic complex morphologies and spatially patterns of the particles. The methodology is efficient and flexible to represent the virtual complex microstructure via different combinations of process parameters. This is particularly important for the property prediction and design of the particle-reinforced composites.

(2) Compared with the simplified-particle model, the 3D microstructure-based model better accounts for the dominant microstructural factors that influence the material properties. Accordingly, the microstructure-based finite element modeling is more accurate in predicting and understanding the macroscopic and microscopic material behavior. The insight into the local micromechanics is also useful for clarifying some material responses that depend on local effects, such as strain-to-failure, fracture toughness, and fatigue life of the composites.

Acknowledgement

The support provided by China Natural Science Foundation (Contract No. 50225517), Shanghai Education Commission Foundation for Excellent Young High Education Teacher (Grant No.YYY08006) and Open Research Foundation of Shanghai Institute of Technology (Grant No.YJ2007-45) is gratefully acknowledged.

References

[1] R. M. Christensen, "A critical evaluation for a class of micromechanics models," *J. Mech. Phys. Solids*, vol. 38, pp. 379–404, 1990.

[2] C. L. Tucker III, E. Liang, "Stiffness predictions for unidirectional short-fiber composites: Review and

evaluation," *Comps. Sci. Technol.*, vol. 59, pp. 655–671, 1999.
[3] S. Torquato, "Modeling of physical properties of composite materials," *Int. J. Solids Struct.*, vol. 37, pp. 411–422, 2000.
[4] R. Mueller, A. Mortensen, "Simplified prediction of the monotonic uniaxial stress-strain curve of non-linear particulate composites," *Acta Mater.*, vol. 54, pp. 2145–2155, 2006.
[5] H. J. Böhm, A. Eckschlager, W. Han, "Multi-inclusion unit cell models for metal matrix composites with randomly oriented discontinous reinforcements," *Comp. Mater. Sci.*, vol. 25, pp. 42–53, 2002.
[6] Jr. L. Mishnaevsky, K. Derrien, D. Baptiste, "Effect of microstructure of particle reinforced composites on the damage evolution: probabilistic and numerical analysis," *Comps. Sci. Technol.*, vol. 64, pp. 1805–1818, 2004.
[7] S. T. Tu, W. Z. Cai, Y. Yin, X. Ling, "Numerical simulation of saturation behavior of physical properties in composites with randomly distributed second-phase," *J. Compos. Mater.*, vol. 39, pp. 617–631, 2005.
[8] J. Segurado, J. LLorca, "Computational micromechanics of composites: The effect of particle spatial distribution," *Mech. Mater.*, vol. 38, pp. 873–883, 2006.
[9] S. R. Annapragada, D. Sun, S. V. Garimella, "Prediction of effective thermo-mechanical properties of particulate composites," *Comput. Mater. Sci.*, vol. 40, pp. 255–266, 2007.
[10] A. Drago, M.-J. Pindera, "Micro-macromechanical analysis of heterogeneous materials: Macroscopically homogeneous vs periodic microstructures," *Comps. Sci. Technol*., vol. 67, pp. 1243–1263, 2007.
[11] Z. Shan, A. M. Gokhale, "Micromechanics of complex three-dimensional microstructures," *Acta Mater*., vol. 49, pp. 2001–2015, 2001.
[12] N. Chawla, V. V. Ganesh, B. Wunsch, "Three-dimensional (3D) microstructure visualization and finite element modeling of the mechanical behavior of SiC particle reinforced aluminum composites," *Scripta Mater*., vol. 51, pp. 161–165, 2004.
[13] N. Chawla, R. S. Sidhu, V. V. Ganesh, "Three-dimensional visualization and microstructure-based modeling of deformation in particle-reinforced composites," *Acta Mater*., vol. 54, pp. 1541–1548, 2006.
[14] L. Babout, E. Maire, J. Y. Buffière, R. Fougères, "Characterization by X-ray computed tomography of decohesion, porosity growth and coalescence in model metal matrix composites," A*cta Mater.*, vol. 49, pp. 2055–2063, 2001.
[15] A. Borbély, P. Kenesei, H. Biermann, "Estimation of the effective properties of particle-reinforced metal-matrix composites from microtomographic reconstructions," *Acta Mater*., vol. 54, pp. 2735–2744, 2006.
[16] N. Chawla, C. Andres, et al., "Effect of SiC volume fraction and particle size on the fatigue resistance of a 2080 Al/SiC_p Composite," *Metall. Mater. Trans.*, vol. 29A, pp. 2843-2854, 1998.
[17] J. Foley, A. van Dam, S. Feiner, J. F. Hughes, R. Philips, "*Introduction to Computer Graphics*," Addison-Wesley publishing company, 1996.
[18] J. N. Goodier, "Concentration of stress around spherical and cylindrical inclusions and flaws," *J. Appl. Mech.*, vol. 55, pp. 39–44, 1933.
[19] K. Wallin, T. Saario, K. Törrönen, "Fracture of brittle particles in a ductile matrix," *Int. J. Fract.*, vol. 32, pp. 201-209, 1986.
[20] J. LLorca, A. Martin, J. Ruiz, M. Elices, "Particulate fracture during deformation of a spray formed metal-matrix composite," *Metall. Trans. A*, vol. 24, pp. 1575-1588, 1993.
[21] W. Weibull, "A statistical distribution function of wide applicability," *J. Appl. Mech.*, vol.18, pp. 293-297, 1951.